Canadian Mineralogist
Vol. 19, pp. 65-82 (1981)

PERALUMINOUS GRANITES PRODUCED BY ROCK–FLUID INTERACTION IN THE RIRIWAI NONOROGENIC RING-COMPLEX, NIGERIA: MINERALOGICAL EVIDENCE

ROBERT F. MARTIN

Department of Geological Sciences, McGill University, 3450 University Street, Montreal, Quebec H3A 2A7

PETER BOWDEN

Department of Geology, University of St. Andrews, St. Andrews, Fife, Scotland KY16 9ST

Abstract

Mildly peraluminous, biotite-bearing granites are spatially associated with fayalite-hedenbergite porphyries and peralkaline granitic rocks in the Ririwai nonorogenic ring-complex, northern Nigeria. The aluminous character of the biotite granites, reflected in micas that belong to the solid-solution series annite-zinnwaldite, appears to develop during a subsolidus episode of mild but pervasive albitization that accompanies disseminated columbite mineralization. The alkali feldspars are transformed into texturally modified perthitic assemblages containing (1) imperfectly ordered microcline instead of orthoclase and (2) ordered albite. The trend culminates in albitites developed along horizontal cooling joints in the roof zone of the granite pluton; the fluid phase here seems to have been more alkaline than the one that caused widespread albitization, as the product is acmite-normative. The Na-enrichment trend is then strikingly reversed along east-west vertical joints; greisenization and K-metasomatism of the wallrocks accompany cassiterite and sphalerite mineralization. Geochemical and isotopic systems are reset during the episodes of interaction with fluid; geochemical data thus cannot be taken at face value to suggest an origin of the peraluminous granites by partial melting of aluminous basement rocks. The biotite granites may represent differentiates of a more basic nonorogenic magma (syenitic or gabbroic) that have been highly modified during their subsolidus, open-system cooling history.

Keywords: nonorogenic granite, Ririwai, Nigeria, ring complex, alkali metasomatism, orthoclase-to-microcline conversion, ion exchange, peraluminous, peralkaline, postmagmatic micas.

Sommaire

Les granites à biotite légèrement hyperalumineux du massif annulaire non-orogénique Ririwai (Nigéria septentrional) sont associés à des porphyres à fayalite et à hédenbergite, ainsi qu'à des granites hyperalcalins. Le caractère alumineux des granites micacés, démontré par l'importance du pôle zinnwaldite dans les biotites annitiques, apparaît à un stade subsolidus, lors d'une albitisation légère mais très étendue qui accompagne une minéralisation en columbite disséminée. Les feldspaths alcalins, modifiés dans leur texture perthitiques, se transforment en assemblages de microcline partiellement ordonnée (aux dépens de l'orthose) avec de l'albite ordonnée. Ce métasomatisme sodique produit des albitites à acmite normative le long de diaclases de refroidissement horizontales à la partie supérieure du massif granitique, où la phase fluide a dû être plus alcaline que celle qui produisit l'albitisation répandue. Le caractère du métasomatisme change ensuite radicalement, lors de la formation de greisens le long des diaclases verticales est–ouest, et c'est le potassium qui se concentre dans l'éponte des greisens à cassitérite et sphalérite. Les systèmes géochimiques et isotopiques se modifient lors des épisodes d'interaction avec solutions hydrothermales. On ne peut donc se fier aux données géochimiques pour conclure que l'anatexie des roches du socle est à l'origine des granites hyperalumineux. Les granites à biotite représenteraient des produits de différenciation d'un magma non-orogénique plus mafique (syénitique ou gabbroïque), fortement modifiés au cours de leur refroidissement subsolidus en système ouvert.

Mots-clés: granite non-orogénique, Ririwai, Nigéria, complexe annulaire, métasomatisme alcalin, transformation orthose–microcline, échange d'ions, hyperalumineux, hyperalcalin, micas post-magmatiques.

Introduction

In debates on the origin of peraluminous granites, a summary statement could be formulated concerning the important role of peraluminous supracrustal material as a contaminant of calc-alkaline magmas or as a source for the anatectic generation of peraluminous liquids in the deep crust. However, such a generalization may not be relevant to the origin of metaluminous and peraluminous biotite granites in certain nonorogenic complexes, where hypersolvus granites seem to have attained peraluminous com-

positions as a result of episodes of subsolidus interaction with fluid. We present here a detailed textural and mineralogical case-study of rocks from the Ririwai ring-complex, Nigeria. Our observations point to an origin of the peraluminous compositions by the removal of alkalis from granites that were initially characterized by the relationship Na + K (+ Ca) $\simeq$ Al.

The Ririwai Nonorogenic Complex

The Younger Granite petrographic province, exposed in Niger and Nigeria, consists in a north–south belt of igneous centres ranging in age from Ordovician [470(5) *Ma* in northern Niger (Karche & Vachette 1976)] to Jurassic [144(2) *Ma* in the most southerly complex in Nigeria]. The ring structures and cupolas represent roots of volcanoes. Igneous activity occurred during three consecutive periods of 50 to 60 *Ma;* for each of these cycles, the igneous centres define an ENE trend (Bowden *et al.* 1976). The eroded volcanic complexes of northern Nigeria (Fig. 1a) are either isolated (*e.g.,* Ririwai, Banke) or coalesced into groups owing to the migration of the centres of magmatism [*e.g.,* Ningi-Burra (Turner & Bowden 1979), Tibchi (Ike 1979)]. These complexes were emplaced in a mixed assemblage of metamorphic and calc-alkaline meta-igneous rocks (*e.g.,* Olarewaju 1978) that yield late Precambrian to Cambrian ages (van Breemen *et al.* 1977). The migmatites and gneisses are considered to be reworked older crustal material. The Younger Granites provide classic examples of intraplate, rift-related magmatism; they are unrelated to any orogeny, and owe their development on a regional scale to thermal anomalies in the mantle.

The Ririwai (or Liruei) complex is located 140 km south of Kano (Fig. 1a). We will focus on this igneous complex because (1) structure and general geology are well described (Jacobson *et al.* 1958, Jacobson & MacLeod (1977); (2) its magmatic and postmagmatic crystallization histories are not influenced by events in neighboring complexes (Fig. 1a), and (3) the biotite granite, dated at 168(2) *Ma* (van Bree-

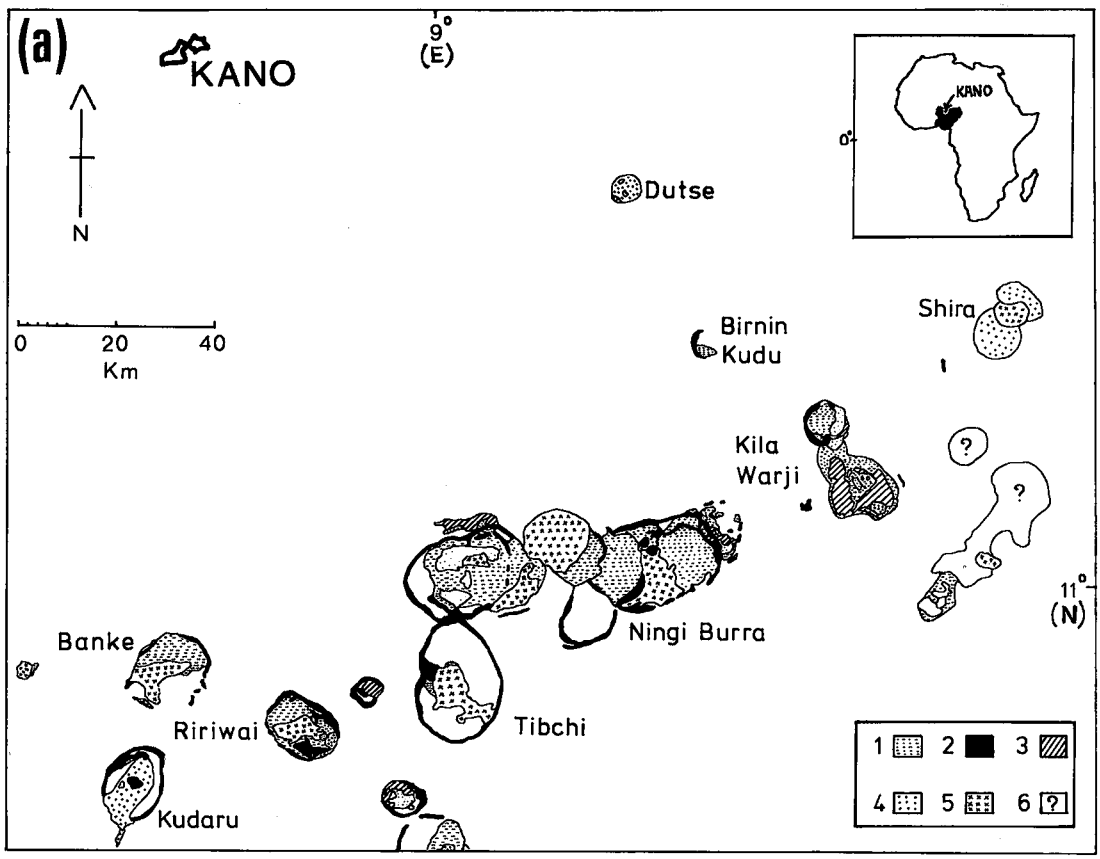

men *et al.* 1975, Bonin *et al.* 1979), is extensively mineralized (see below). No *major* tectonic events have occurred in the area since Jurassic times.

Smith & Bailey (1968) considered Ririwai an excellent example of a resurgent subvolcanic cauldron. Precaldera ignimbritic units and minor flows are preserved in the collapsed caldera.

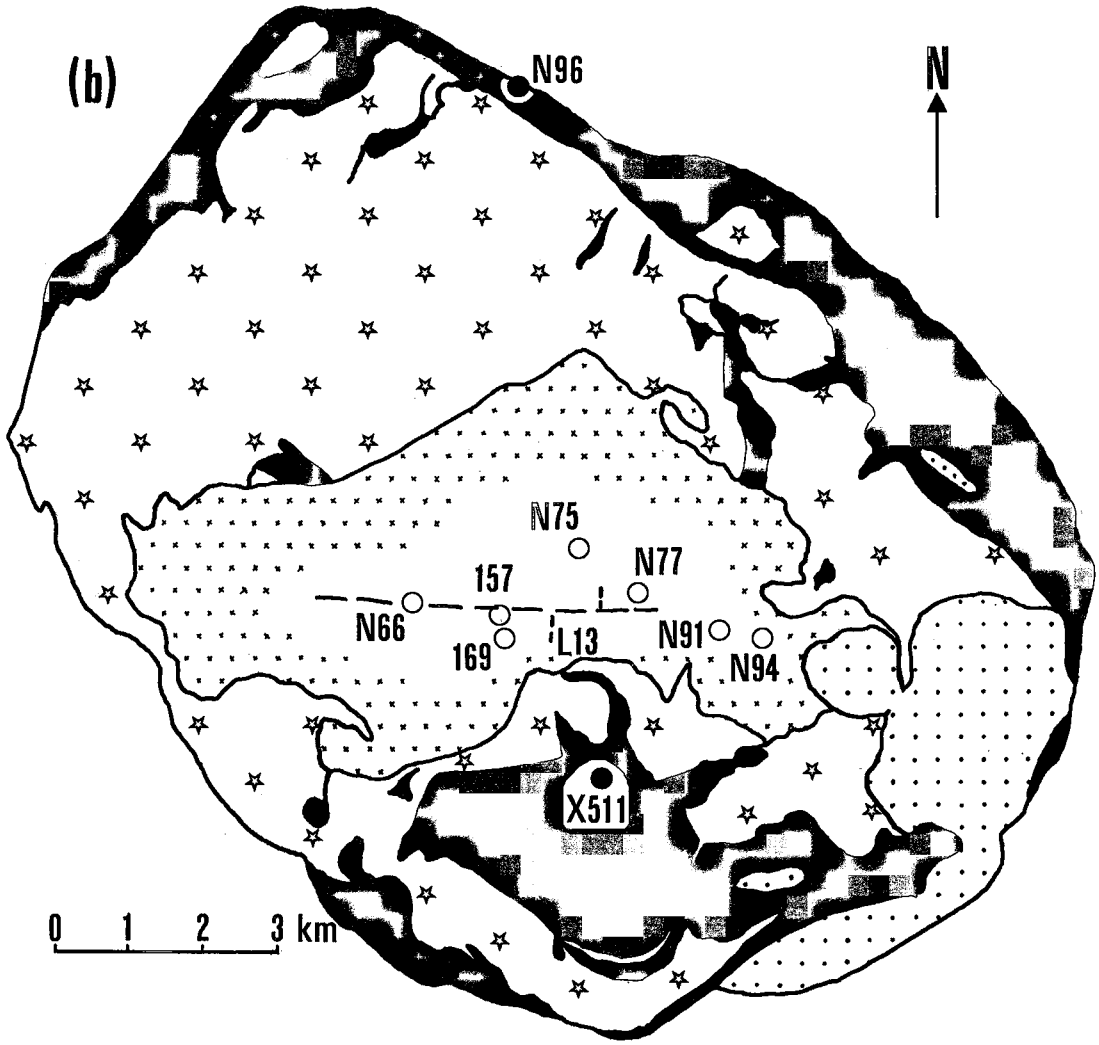

FIG. 1. (a) Geological sketch-map of the northern ring-complexes of Nigeria. (1) volcanic rocks, dominantly pyroclastic in origin; (2) porphyries, granite porphyries, granites emplaced as sheets, ring dykes and plugs; these rocks contain fayalite, hedenbergite ± Na–Ca or Na amphibole ± biotite; (3) syenite (absent at Ririwai except for metasomatized variants of the biotite granite: see text); (4) peralkaline granite containing ferroricherite or arfvedsonite; (5) biotite granite and microgranite; (6) complexes not mapped in detail. Information on Shira, Dutse, Birnin Kudu complexes from J.N. Bennett (1981); Ningi–Burra was studied by Turner & Bowden (1979), and Tibchi by Ike (1979). The map of other complexes is simplified from an original compilation by D.C. Turner based on records and bulletins of the Geological Survey of Nigeria. (b) The map of Ririwai is taken from Jacobson & MacLeod (1977). Specimen numbers shown are those mentioned in the text; 157 and 169 refer to 77–157 and 77–169, respectively. The E–W dashed line is the Ririwai lode; L13 is a borehole that intersects it. Closed circles: unit 2 (X511 in the Dutsen Shetu plug, N96 in the ring dyke); open circles: unit 5. Unit 1 is here shown by a star pattern.

Jacobson & MacLeod (1977) recognized several postcaldera vent complexes and a ring dyke of fayalite granite porphyry (2 in Fig. 1). These units provide a valuable sample of the gas-poor magma that emerged after explosive evacuation of the upper portions of the zoned reservoir (1, Fig. 1). Peralkaline granites and mildly aluminous, biotite-bearing granites (4 and 5, respectively, on Fig. 1) then were intruded, though their interrelationship and the sequence of emplacement remain controversial. The biotite granites cover approximately 25% of the 134-km² complex, and the unit may widen with depth (Jacobson & MacLeod 1977, Table 20, Plate 6; Ajakaiye 1968). Unit 5 is important not only in volume: at Ririwai and in neighboring complexes, the biotite granites contain disseminated columbite and also host Zn, Sn mineralization along a system of east–west greisenized fissures (Fig. 1b; Bowden & Kinnaird 1978).

Jacobson & MacLeod (1977) proposed two diverging trends of evolution at Ririwai: a "normal" series (leading to peraluminous biotite granite) and an alkaline series (unit 4), both issued from a common granitic parent magma, itself a derivative of a tholeiitic magma. Whether or not this divergence occurred entirely at the magmatic stage, as advocated by Jacobson & MacLeod, or as a result of metasomatic overprints remains an important and thorny question. Such a bifurcation at the end stages of magmatic evolution certainly is difficult to explain, especially as signs of crystal accumulation (a process advocated by Jacobson & MacLeod) or of obvious contamination by the host rocks are exceedingly rare. In this paper, we examine rocks that constitute the normal series at Ririwai. The two specimens selected from unit 2 may be taken as representative of quenched granitic liquids, though even these specimens show mild *increase* in alkalinity, which most likely occurred at the deuteric stage (see below). The magmas that congealed to give rocks of unit 5 were located stratigraphically below those that rose in the ring dyke and in the feeder zone (unit 2). We defer discussion on the evolution of the alkaline series at Ririwai.

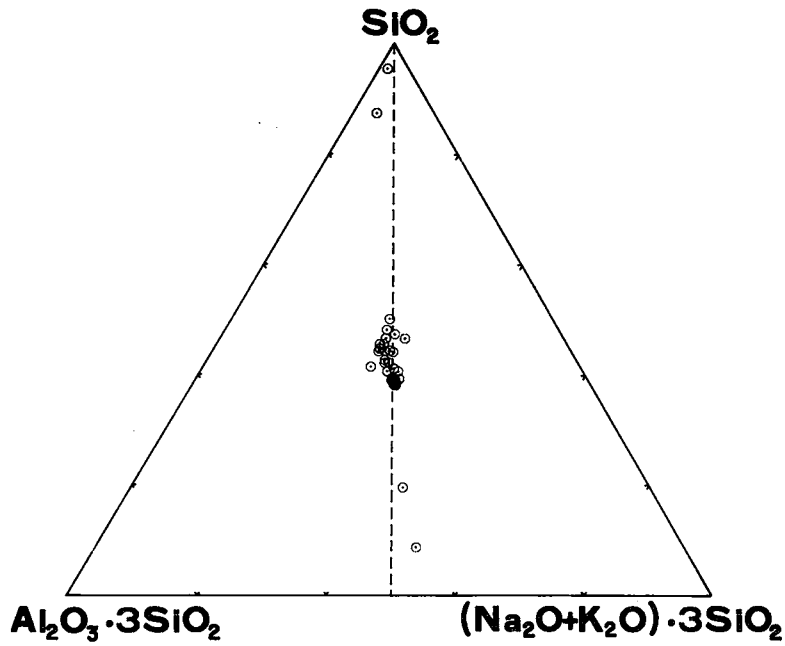

FIG. 2. Triangular plot of available analyses of biotite granite from Ririwai in terms of SiO_2, $Al_2O_3 \cdot 3SiO_2$ and $(Na_2O+K_2O) \cdot 3SiO_2$. The dashed line expresses the relationship $Na+K = Al$. The two closed circles represent X511 and N96 (both from unit 2), considered closely representative of the evolved parental magma to rocks of units 2. Source of analyses: Jacobson & MacLeod (1977), Abaa (1976), Table 1 and unpublished data. Albite and K-feldspar plot at the intersection of the dashed line and the base of the triangle.

Petrography and Composition of the Units that Define the "Normal" Series

The spectrum of rocks to be considered ranges from quartz–pyroxene–fayalite porphyry (unit 2) to biotite granite and strongly metasomatized variants (unit 5). We contend that a full understanding of the "normal" series can emerge only from careful petrographic observations and a ranking of the rocks, from pristine (magmatic) to increasingly disturbed in texture and composition owing to postmagmatic reactions.

The quartz–pyroxene–fayalite porphyries of the Dutsen Shetu vent complex (unit 2)

Dutsen Shetu is the largest resurgent dome at Ririwai; it consists of 7 km² of porphyry and a 13 km² envelope of agglomerate and intrusion breccia (Fig. 1b, large area of unit-2 rocks in the south-central part of the complex). In terms of the overall development of the Ririwai complex, this plug constitutes a spine of relatively viscous degassed rhyolitic material that rose in a vent through the products of early volcanism (Smith & Bailey 1968). The plug consists largely of hard, vesicle-free black porphyries that must have been porphyritic obsidians; as a result of its hardness, the spine constitutes the highest and most inaccessible points of the complex (1225 m and many crests above 1075 m). The specimen descriptions of Jacobson *et al.* (1958) and Jacobson and MacLeod (1977) suggest strongly that little has happened since the emplacement to modify the feldspars and the microphenocrysts of hedenbergitic clinopyroxene and fayalite. Specimen X511, a dark green porphyry, may be considered closely representative of the original, unmodified magma near the top of the reservoir; its composition (Jacobson *et al.* 1958, Table XI; closed circle in Fig. 2) plots in a central position in the diagram $Al_2O_3 \cdot 3SiO_2$–$(Na_2O+K_2O) \cdot 3SiO_2$–$SiO_2$, very close to the vertical line Na + K = Al. Specimen X511 contains numerous tabular Carlsbad-twinned phenocrysts (< 5 mm) of "pale green glassy orthoclase" (Jacobson *et al.* 1958, p. 32). Jacobson & MacLeod (1977, p. 65) concluded, on the bases of $2V$ and a partial chemical analysis, that the feldspar is an apparently homogeneous member of the sanidine–anorthoclase series. Feldspar crystals enclose microphenocrysts of clinopyroxene and fayalite. The microcrystalline matrix contains quartz, perthitic feldspar and a poikilitic Na–Ca amphibole that mantles the primary ferromagnesian phases. Jacobson and coworkers also noted irregular cloudy zones that cross and rim the feldspar phenocrysts (see below).

The peripheral ring dyke of granite porphyry (unit 2)

The ring dyke provides yet another opportunity to obtain pristine specimens that are closely representative of the degassed granitic magma that rose as the caldera collapsed (Fig. 1b). Ring-dyke rocks vary widely in grain size of the groundmass and in the importance of black, aphanitic, rounded xenoliths. Close to the contact with the Precambrian basement, for example, we have found areas of dark green to black, devitrified, highly porphyritic obsidian very similar in mineralogy and textural development to X511. Where the rate of crystallization was slower (or devitrification and recrystallization were more complete), the matrix is light grey and microgranitic in texture; however feldspar compositions are similar. In specimen N96, from the north side of the complex (Fig. 1b), the brown feldspar phenocrysts are mantled by a narrow bleached rind and transected by a network of subparallel bleached fissures $\perp$ (010) that subdivide the grain into relics of clear brown alkali feldspar. In thin section, these domains seem cryptoperthitic (*i.e.*, free of visible lamellae), unaltered and untwinned; the bleached fissures and rims appear as turbid areas in which the feldspar is cracked along its principal cleavages and riddled with indeterminate high-relief inclusions (Fig. 3). Locally, the turbid feldspar shows polysynthetic twin-

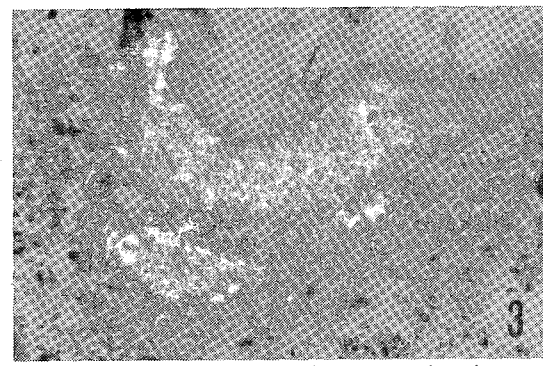

Fig. 3. Development of turbidity around and across orthoclase cryptoperthite phenocryst in X511, Dutsen Shetu porphyry (unit 2). The zones of turbidity contain fine acicular wisps of alkali-bearing amphibole, as does the turbid groundmass assemblage. Plane-polarized light; width of field of view is 0.8 mm. Similar feldspars are found in specimens of the ring dyke (*e.g.*, N96, as described in the text).

ning, though the width of individual twin lamellae is highly variable. In the groundmass, the equant feldspar grains are invariably turbid (Fig. 3); differences in extinction angles suggest that each grain consists of a central area of apparently untwinned turbid K-feldspar mantled and veined by sparsely and irregularly twinned albitic feldspar.

The increase in volume of turbid feldspar is clearly paralleled in the complex assemblage of mafic minerals. Microgranite porphyry N96 contains microphenocrysts of fayalite and hedenbergitic clinopyroxene, commonly in contact with the orthoclase cryptoperthite phenocrysts (see below). Fayalite typically has altered in part to grunerite and magnetite, and the ferrohedenbergite is rimmed by a zone of green sodic ferrohedenbergite. Aegirine fills fractures that postdate the formation of the bleached, albite-rich cracks in the orthoclase perthite. Surrounding the olivine pseudomorphs and the green-rimmed ferrohedenbergite, and forming the dominant mafic mineral in N96, are clusters of green- to blue-fringed Na–Ca- to Na-bearing amphiboles. These vary from ferrowinchite (core) to ferrorichterite to arfvedsonite (rim), according to preliminary microprobe information. Wisps of arfvedsonite also occur within the turbid feldspars (Fig. 3), but not in the fresh feldspar. The clusters of amphibole also enclose grains of titanomagnetite; also, annitic mica has formed at the expense of the magnetite in N96.

On textural and mineralogical grounds, we believe that N96 contains a record of (1) magmatic, (2) late magmatic to early postmagmatic and (3) later postmagmatic episodes of crystallization. In particular, we suggest that the arfvedsonite, annite, grunerite, aegirine and magnetite (from fayalite breakdown) formed at subsolidus temperatures (a) at the site and at the expense of the initial mafic mineral assemblage, (b) within the turbid, porous groundmass feldspars and (c) within the turbid outer portions of the orthoclase phenocrysts. The processes of postmagmatic recrystallization seem to have occurred over a longer time span (slower cooling?) in N96 than in X511; as in X511, however, the indicators of peralkalinity made their appearance at subsolidus temperatures.

TABLE 1. CHEMICAL ANALYSES OF RIRIWAI GRANITE PORPHYRY (UNIT 2, N96) AND BIOTITE GRANITES (UNIT 5)

	N96	N75	N77	N78	N79	N91	N92	N94
SiO_2	72.40	75.86	76.80	77.90	76.27	75.91	76.27	75.57
TiO_2	0.28	0.11	0.07	0.04	0.07	0.10	0.12	n.d.
Al_2O_3	12.35	12.85	11.99	11.86	12.29	12.71	12.54	13.92
Fe_2O_3	1.58	0.33	0.47	0.18	0.55	0.39	0.24	0.43
FeO	2.30	1.05	0.97	1.17	1.02	1.12	1.21	1.07
MnO	0.09	0.05	0.03	-	0.02	0.03	0.03	0.05
MgO	0.05	0.02	0.01	0.02	0.03	tr.	0.01	0.01
CaO	0.76	0.24	0.24	0.44	0.32	0.16	0.22	0.26
Na_2O	4.44	3.91	3.92	3.95	3.81	3.72	3.74	3.84
K_2O	4.87	4.30	4.31	4.19	4.50	4.50	4.33	4.41
P_2O_5	0.04	tr.	tr.	0.01	0.01	tr.	tr.	0.01
H_2O^+	0.24	0.46	0.17	0.24	0.33	0.24	0.32	0.27
H_2O^-	0.13	0.06	0.05	-	0.08	0.09	0.15	0.10
total	99.29	99.24	99.03	100.00	99.30	98.97	99.18	99.94
A/CNK	0.89	1.12	1.04	1.00	1.05	1.13	1.12	1.20
D.I.	91.2	93.9	95.0	95.2	93.5	94.1	93.9	93.6

Analyst: Richard Batchelor, Department of Geology, University of St. Andrews. D.I.: $\Sigma(Q + Ab + Or)$. A/CNK = $Al_2O_3/(CaO + Na_2O + K_2O)$, defined on a molar basis.

In terms of composition (Table 1), specimen N96 (second closed circle in Fig. 2) greatly resembles X511; both are now slightly alkaline, but lie very close to the vertical line Na + K = Al. In view of the distribution of alkaline minerals in N96, the granitic *magma* may have been characterized by Na + K (+Ca) $\approx$ Al. Approximate bulk compositions of the feldspars are given in Figure 4.

The biotite granites and the greisens (unit 5)

In nonorogenic granites the molar ratio $Al_2O_3/(CaO+Na_2O+K_2O)$ [abbreviated A/CNK], by which the peraluminous character is normally gauged, converges to the ratio $Al_2O_3/(Na_2O+K_2O)$. Most biotite granites at Ririwai contain much less than 1 wt. % CaO, and much of that calcium is tied up in CaF_2 (usually demonstrably secondary). For example, in biotite granite X568 (0.35% F, 0.51% CaO: Jacobson & MacLeod 1977, Table 7), the ratio A/CNK (1.01) becomes 1.09 (*i.e.*, = A/NK) when a correction is made for Ca in fluorite. Because values of F are not available for some of the 27 rocks analyzed (see Table 1), the results of all available analyses are plotted in the Ca-free system, in terms of the components $(Na_2O+K_2O)\cdot 3SiO_2$–$Al_2O_3\cdot 3SiO_2$–SiO_2 (Fig. 2), to illustrate their aluminous character. Almost all specimens from unit 5 are mildly peraluminous, plotting to the left of the vertical line Na+K = Al.

The central stock of biotite granite has shallow-dipping centripetal contacts and forms a cupola, emplaced high into the overlying volcanic pile. The biotite granite is without volcanic equivalents at Ririwai. The unit has been arbitrarily split by Jacobson & MacLeod (1977) into medium- and coarse-grained varieties, but there exists a range of biotite-bearing medium- to coarse-grained granites that possess subtly porphyritic to equigranular textures. Much of the mass of biotite granite at Ririwai has been affected by hydrothermal activity and disseminated columbite mineralization. In specimens N91, N75 (Table 1; A/CNK = 1.13 and 1.12, respectively) and many of the borehole specimens from the centre of the unit, columbite is

the only abundant accessory opaque mineral. Rocks of unit 5 also host the largest Zn-Sn mineralized vein system in Nigeria. It strikes east–west for over 5 km across the centre of the biotite granite (Fig. 1b) and extends to depths of 300 m, on the basis of borehole studies. This lode is essentially vertical, and consists of a series of narrow, braided quartz veins with greisen borders and zones of red to pink wallrock alteration from 1 to 8 m in width. The intensity of hydrothermal mineralization at Ririwai can be measured by the high production figures for alluvial cassiterite and columbite, and by the government's recent decision to develop the first underground tin mine in Nigeria. The biotite granite we now see in hand specimen represents the result of successive waves of rock–fluid interaction; in many instances, the magmatic assemblage has been almost completely obliterated.

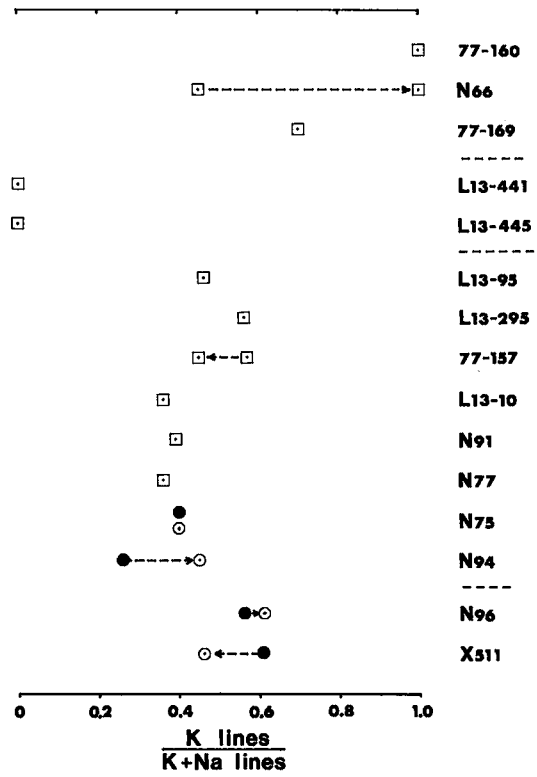

FIG. 4. One possible ranking scheme of the specimens of unit 5 examined in this study, based on degree of order, composition and textural development of the feldspars examined. Bulk composition is estimated by the proportion of the total feldspar diffraction lines in the angular interval 12° to 65° 2θ (Cu $K\alpha_1$ radiation) that are attributed to K-feldspar. Specimens X511 and N96 represent unit 2; specimens N94 and N75 are porphyritic rocks of unit 5. In these four porphyritic rocks, the phenocryst assemblage is represented by a closed circle, matrix by an open circle (hence the direction of the arrow). The feldspar assemblage of equigranular rocks is represented by an open square. The most strongly metasomatized rocks in unit 5 appear towards the top of the diagram. The four groups of rocks, separated by dashed lines, are: Unit 2, Unit 5 (slightly metasomatized), Unit 5 (strongly Na-metasomatized), Unit 5 (K-metasomatized).

One of the texturally most pristine specimens of unit 5 in our collections is N94, a peraluminous hypersolvus granite (Table 1; A/CNK = 1.20) that outcrops roughly midway between the eastern end of the greisen-vein system and the peralkaline granites of unit 4 (Fig. 1b). The porphyritic rock contains paramorphs after β-quartz and pale greenish-grey euhedral perthite as phenocrysts up to 8 mm across. The braid-like, regularly alternating lamellae of K- and Na-feldspar in the phenocryst are what one might expect to result from exsolution of an originally homogeneous sanidine.

The whitish, slightly hematite-stained groundmass of N94 is mineralogically quite different from the phenocryst assemblage: it consists of equigranular perthite, anhedral quartz and biotite grains. The feldspars are not braided but show a patch pattern, with coalesced domains of more turbid K-feldspar and fresh-looking albite that occurs preferentially near the grain

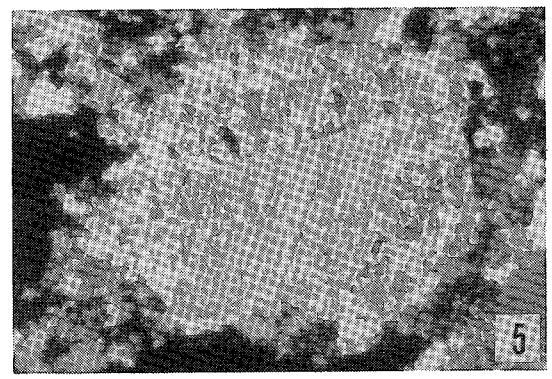

FIG. 5. Mildly albitized perthite grain in biotite granite N77. Certain areas near the centre of the crystal contain a typical regular alternation of perthitic lamellae of probable exsolution origin. In the outer parts of the grain, the intergrowth has coarsened and consists of coalesced irregular domains of intermediate microcline (dark grey) and albite (white). Crossed nicols; width of field of view is 3.3 mm.

margins. The biotite invariably is interstitial, micropoikilitic, and associated with the albite component of the disturbed perthite. Many other specimens of unit 5 in our collections (*e.g.*, N75 and N77, Fig. 1b) are biotite-bearing, medium- to coarse-grained and peraluminous; texturally, they range from subtly porphyritic to equigranular. They are characterized by perthitic alkali feldspars that are partly to completely disturbed, in terms of the distribution of K-rich and Na-rich domains (Fig. 5); the volume of albite exceeds that of K-feldspar, according to the number of diffraction peaks measured (Fig. 4). The apparently untwinned K-feldspar is consistently turbid. Finally, the coarse grained biotite granites (*e.g.*, N91, L13–10 and L13–295, Fig. 1b) are whitish, relatively friable and locally stained with hematite. Here, the distribution of the turbid K-feldspar is very patchy, and the volume of Na-feldspar predominates over that of K-feldspar (Fig. 4). We contend that these biotite granites have undergone Na-for-K exchange. This transformation probably accounts for the generally poor exposure of this unit: ion exchange of Na for K leads to an 8% reduction in the molar volume of an alkali feldspar, which causes a weakening of individual feldspar grains, an increase in porosity and a significant decrease in its physical resistance.

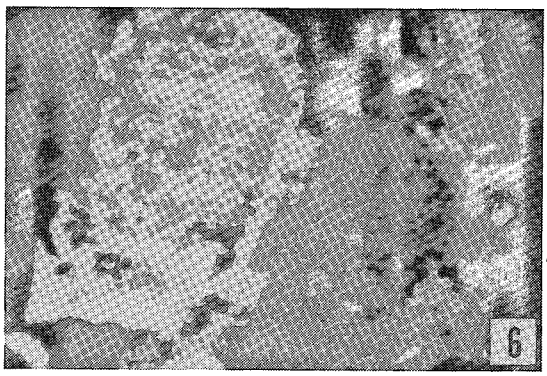

FIG. 6. An example of more highly modified perthite texture in biotite granite L13–95. There has been important Na-for-K ion exchange that accompanied disseminated columbite mineralization. A flake of aluminous biotite can be seen immediately to the left of the number 6, in intimate contact with the more highly disturbed parts of a perthite grain. Vestiges of the original Carlsbad twin composition plane remain in the perthite grain to the left; all the K-feldspar (intermediate microcline) has coalesced into domains, which are now free of albite lamellae. Crossed nicols; width of field of view is 3.3 mm.

As in many other nonorogenic granites, the pegmatitic end-stages of magmatic crystallization are amazonite-bearing (Foord & Martin 1979). Specimen 77–157 contains pegmatitic clots in which the perthite is green. The green color is due to structurally bound Pb; a spectrographic analysis of the green material gave 700 ppm Pb, 300 ppm Ga, 5000 ppm Rb and 15 ppm Cs (E.E. Foord, pers. comm. 1980). These grains are cross-cut and rimmed by a butter-colored microcline perthite pseudomorph. Such pegmatitic clots generally are associated with fine-grained, microgranitic patches encountered at various intervals along the exploratory ramp near the Sn–Zn lode (D. Hanneford, pers. comm. 1977). These microgranites commonly contain acicular biotite, here interpreted (by the first author) as pseudomorphic after an alkali amphibole. If confirmed in future investigations, this inference would indicate that some of the rocks now mapped as unit 5 once had affinities with unit 4. Late transformations may thus have confused the field relationships between rocks of units 4 and 5.

Light greenish-grey microgranitic bands also occur repeatedly in medium- to coarse-grained biotite granite along borehole L13 (Fig. 1b). These bands are considered largely to reflect major recrystallization associated with the introduction of disseminated columbite. In the feldspar grains of specimen L13–95 (Fig. 6), the potassium-rich domains are dusty, apparently untwinned, and have entirely coalesced to give a crude zonal pattern. Clear albitic feldspar

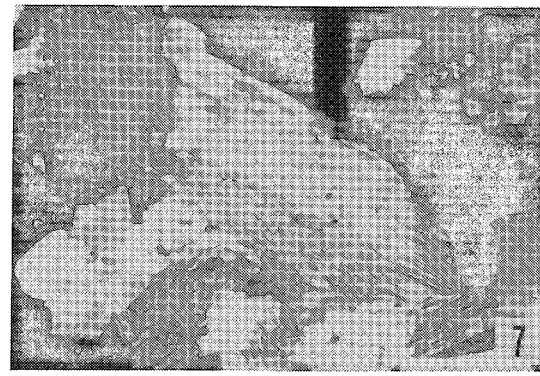

FIG. 7. An example of extreme albitization: albitite L13–445. The original grain of perthite is now represented by the array of small-scale albite domains. An overgrowth of albite of hydrothermal origin is free of dustlike inclusions and has a much wider spacing of twin lamellae. The overgrowth preserves the orientation of the original Carlsbad twin composition plane. Crossed nicols: width of field of view is 3.3 mm.

surrounds the K-rich islands and rims the grains; with it are associated fluorite and a fresh aluminous biotite (*i.e.*, to the left of "6" in Fig. 6).

In a number of bands along the 451-m length of hole L13, and especially below 350 m, Na-for-K exchange has reached completion, and the quartz has been removed, either in part (L13–445) or completely. The resulting feldspathic rocks may be very vuggy; the vugs are commonly coated with hydrothermally deposited albite. In L13–441, an albitite, the feldspar grains consist entirely of chequered albite-twinned domains. Trains of inclusions mimic the original perthitic texture, but no K-bearing feldspar remains (Fig. 4). Relict Carlsbad composition planes are now partly obliterated (Fig. 7); the rims on the albite pseudomorphs show no domain texture, no dusting, and more widely spaced twin lamellae. A green mica seems to postdate albitization. The fluids that caused this extreme degree of sodium metasomatism must have been peralkaline, as the resulting feldspathic rocks have agpaitic indices greater than 1.0 (Fig. 2). Abaa (1976) reported values of 1.18 and 1.10 for specimens L13–411 and L13–440, respectively.

Several samples collected within the east–west system of braided quartz veins with greisen borders and reddish alteration envelopes have also been examined. The specimens of reddened biotite granite contain very turbid, brick-red K-feldspars partly converted to quartz, Li-, Fe-bearing mica and topaz (Jacobson & MacLeod 1977). Vuggy pink quartz-free rocks that texturally resemble the albitites described earlier have been encountered near the alteration aureole next to the braided quartz veins. These rocks (*e.g.*, 77–169, Fig. 1b) are similar in certain respects to the episyenites described from uranium-mineralized zones in the Massif Central (Leroy 1978). They contain euhedral cassiterite [*a* 4.7370(4), *c* 3.1851(3) Å] and tiny transparent spheres of fluorite that partly fill some of the cavities. Specimen 77–160 is best termed a sphalerite episyenite in which K-for-Na exchange is complete (Fig. 4). The dominance of microcline in the zone of wall-rock alteration and the appearance of "microclinites" (see below) suggest that the earlier trend of Na-for-K ion exchange associated with columbite mineralization clearly was reversed during cassiterite + sphalerite mineralization. K-for-Na ion exchange seems to be the dominant lower-temperature process along zones of wallrock alteration and greisenized fractures belonging to the Ririwai lode. The efficient removal of sodium from this zone, noted by Jacobson (1947) and Abaa (1976, 1978), is recorded in the feldspar assemblage; the tin and zinc may have been transported as alkali-bearing complexes that became supersaturated in the temperature range 400–250°C (Bowden & Kinnaird 1978).

The Feldspars

Because these granitic rocks are poor in calcium, and because Ca is partitioned amongst minerals like fluorite, apatite, amphibole, clinopyroxene as well as feldspar, it is appropriate to consider the alkali feldspars in the Ririwai rocks in terms of the system $NaAlSi_3O_8$–$KAlSi_3O_8$ and the pertinent equilibrium phase diagram. Information on composition N_{Or} and degree of Si–Al order in the coexisting feldspars is obtained from unit-cell parameters, computed using indexed 2θ reflections as input for the cell-refinement program of Appleman & Evans (1973). A spinel standard (a = 8.0833 Å at room temperature) serves to correct the diffraction pattern, obtained with a Guinier–Hägg focusing camera (Cu $K\alpha_1$ radiation). Composition may be inferred from unit-cell volume (Stewart & Wright 1974) and was checked by microprobe data for selected specimens. The degree of Si–Al order, obtained from b, c, α^* and γ^* using the formulation of Blasi (1977), is expressed by t_1O, the proportion of Al in the T_1O position. A quenched magmatic feldspar is expected to be disordered (t_1O = 0.25) and compositionally intermediate between the Na and K end-members. Feldspars that have equilibrated during a low-temperature event will contain triclinic Na-poor microcline and pure albite (t_1O = 1.0 in both cases). Cell dimensions are listed in Table 2, which may be obtained from the Depository of Unpublished Data, CISTI, National Research Council of Canada, Ottawa, Ontario K1A 0S2. Calculated values of N_{Or} and of the inferred proportion of Al in the T_1 position in each feldspar studied are presented in Table 3. Attempting to reconstitute the original magmatic feldspar composition by homogenizing the observed assemblage was judged futile in view of the importance of ion-exchange processes during low-temperature events at Ririwai, as illustrated in the previous section.

Our brief petrographic notes and the thorough descriptions of Jacobson *et al.* (1958) and Jacobson & MacLeod (1977) hint at a spectrum of feldspar compositions and structural states that spans magmatic to low-temperature hydrothermal events. The rocks mentioned above are examined in turn.

TABLE 3. INDICATORS OF COMPOSITION AND DEGREE OF Si-Al ORDER IN RIRIWAI FELDSPARS, UNITS 2 AND 5

		N_{Or}	Δbc	$\Delta\alpha^*\gamma^*$	t_1O	Δ	#	N_{Or}	Δbc	$\Delta\alpha^*\gamma^*$	t_1O	ψ	#
		K-rich feldspar						Na-rich feldspar					
Unit 2: the Dutsen Shetu vent complex													
X511	phenocryst	0.950	0.776	0	0.388	0	30	-0.031	0.972	0.979	0.975	1.100	19
	matrix†	0.968	0.755	0	0.377	0	26	-0.017	0.985	0.944	0.964	1.113	30
Unit 2: the peripheral ring-dyke													
N96	phenocryst	0.965	0.794	0	0.397	0	23	-0.001	1.035	0.933	0.984	1.179	18
	matrix	0.992	0.998	0.557	0.778	0.692	23	-0.012	0.944	0.938	0.941	1.103	15
Unit 5: the biotite granites and metasomatized derivatives (least → most disturbed; see Fig. 4)													
N94	phenocryst	0.975	0.722	0	0.361	0	8	-0.020	0.983	0.987	0.985	1.103	23
	matrix	0.948	0.981	0.850	0.916	0.826	20	-0.026	0.972	0.972	0.972	1.125	24
N75	phenocryst	0.947	0.949	0.767	0.858	0.809	17	-0.022	0.992	0.986	0.989	1.115	26
	matrix	0.945	0.955	0.774	0.864	0.780	14	-0.018	0.999	0.979	0.989	1.095	21
N77		0.989	0.936	0.766	0.851	0.706	16	-0.013	1.003	0.981	0.992	1.097	28
N91		0.981	0.993	0.758	0.876	0.808	14	-0.022	0.997	0.987	0.992	1.109	22
L13-10		0.961	0.993	0.781	0.887	0.772	15	-0.019	0.974	0.948	0.961	1.134	27
77-157	green	0.941	0.843	0	0.421	0	25	-0.018	0.976	0.961	0.968	1.112	31
	(amazonite)	0.917	0.877	0.714	0.795	0.500	16						
77-157	cream	0.962	0.972	0.904	0.938	0.892	47	-0.014	0.998	0.989	0.994	1.101	44
L13-295		0.955	0.966	1.042	1.004	0.914	28	0.016	0.994	1.006	1.000	1.099	22
L13-95		0.978	1.038	0.961	0.999	0.919	27	-0.019	0.966	0.988	0.977	1.100	32
L13-445		K-feldspar is absent						-0.018	0.948	0.990	0.969	1.112	40
L13-441								-0.010	0.989	0.980	0.985	1.103	29
77-169		1.009	0.975	0.880	0.927	0.890	47	-0.010	0.983	0.959	0.971	1.037	20
N66	pink	0.997	1.011	0.822	0.917	0.785	22	-0.005	1.003	0.989	0.996	1.119	27
N66	red	0.994	0.979	0.950	0.950	0.926	21	Albite is absent					
77-160		0.967	0.988	0.960	0.974	0.945	62						

† a trace of intermediate microcline is present in the matrix of X511. The sequence of presentation is the same as in Figure 4, i.e., from the most pristine to the most strongly metasomatized, keeping in mind the temporal relationships (K-metasomatism follows Na-metasomatism). Composition N_{Or} is calculated from unit-cell volume, formulation of Stewart & Wright (1974); Δbc (= $t_1O + t_1m$) is obtained by the program of Blasi (1977), as is $\Delta\alpha^*\gamma^*$ (= $t_1O - t_1m$). The obliquity of a triclinic K-feldspar Δ is $12.5(d_{131} - d_{1\bar{3}1})$; in a plagioclase, ψ is the angular separation $2\theta_{131} - 2\theta_{1\bar{3}1}$, in degrees. Specimens are identified in the text. # refers to the number of diffration lines used in the cell refinement (program of Appleman & Evans 1973).

The quartz–pyroxene–fayalite porphyries (unit 2)

The phenocrysts in X511, from Dutsen Shetu, consist largely (~ 95% by volume) of greenish cryptoperthitic orthoclase, characterized by an average composition N_{Or} of 0.96 (1.0 for pure $KAlSi_3O_8$) and a degree of Si–Al order typical of common orthoclase ($t_1O = t_1m = 0.39$). Each greenish phenocryst is crossed by conspicuous white lines that are traces of cracks in the crystal. In thin section, these lines show up as areas of turbidity developed along a system of roughly parallel cracks that do cross the Carlsbad twin plane. However, the cracks taper and die off in the second individual; they may thus have originated by thermal contraction. The turbid lining of these cracks contains *microperthitic* intergrowths of orthoclase and albite; these coarser intergrowths have evidently formed by local recrystallization of cryptoperthite along cracks. In X511, these turbid linings are connected with a partial rim of the same material around many of the phenocrysts (*e.g.*, Fig. 3). In contrast, *all* feldspar grains in the fine grained groundmass of X511 are of the turbid, microperthitic type. The predominance, in the groundmass assemblage, of albite over orthoclase (comparable in degree of Si–Al order to the cryptoperthite orthoclase: Table 3, Figs. 4, 8) suggests that the coarsening of the perthitic texture probably was here accompanied by moderate Na-for-K exchange (hence the arrow in Fig. 4). Interestingly, the powder pattern of the groundmass assemblage also contains the strongest diffraction lines of structurally intermediate microcline. Finally, the primary ferromagnesian mineral assemblage in X511 shows complementary changes: where trapped as inclusions within the homogeneous-looking, cryptoperthitic orthoclase, microphenocrysts of olivine and clinopyroxene are fresh and intact. However, most of these microphenocrysts occur in the groundmass, where they show overgrowths of a sodic-calcic amphibole and annite; sodic-calcic and arfvedsonitic amphibole occurs in cellular and micropoikilitic grains, with separate patches in optical continuity. Also widespread in the matrix, and occasionally within turbid areas of phenocrysts, are wisps and acicular prisms of similar amphibole (Fig. 3).

The data presented for the phenocrystic feldspar in porphyry N96 from the ring dyke (Table 3, Fig. 8) indicate that the K-feldspar is relatively pure, well-ordered orthoclase: $N_{Or} = 0.965$, $t_1O = 0.40$. This degree of Si–Al order exceeds what is expected in very fresh rhyolites and, as in X511, approaches the maxi-

mum that can be expected of a "monoclinic" feldspar. Coexisting with orthoclase in the white rims, along bleached fissures and presumably also as true exsolution lamellae within the cryptoperthitic orthoclase, is high-purity albite (N_{Or} = 0: Table 3). The cell constants of this feldspar, in particular its β^* and γ^*, are consistent with ordered, calcium-free albite, so that the apparent slight departure from complete Si–Al order (t_1O = 0.98) does not seem to be caused by Ca in the structure.

In contrast to the phenocrysts, where *orthoclase cryptoperthite* is dominant, the equant turbid grains in the microgranitic groundmass of N96 consist of an assemblage of *intermediate microcline* (t_1O = 0.76, $\triangle$ = 0.69, N_{Or} = 0.99; Fig. 8) and *albite* of high purity, apparently departing slightly from complete Si–Al order (t_1O = 0.94). We infer that the whitish turbid material that surrounds and crosses the brown orthoclase perthite phenocrysts in N96 also contains intermediate microcline. In view of the restricted field of stability of microcline (below 450°C: Smith 1974, Fig. S–1), the rocks selected as samples of unit 2 show incipient (X511) to partial (N96) conversion to a low-temperature assemblage. The structural conversion is incomplete even in the groundmasses, where the large surface area of the feldspar grains would favor efficient exchange with an interstitial aqueous fluid. Compositionally, the feldspars in the two specimens probably equilibrated below 300°C, in view of their high purity.

One of the most pristine specimens of unit 5 (N94) contains orthoclase and lamellae of low albite in the phenocrysts. The orthoclase has a lower degree of Si–Al order than that in the two porphyries from unit 2: t_1O = 0.36 (Table 3). It is among the most disordered feldspars to be found at Ririwai; this may mean that N94 cooled too rapidly for efficient Si–Al ordering to occur in the phenocrysts. As in N96 of unit 2, however, the conversion to microcline is complete in the matrix (t_1O = 0.91, $\triangle$ = 0.83). Detailed XRD analyses are required to identify the K-feldspar as microcline, as the grains appear untwinned; the scale of the grid pattern may be submicroscopic, as it is an expected sign of the conversion of a monoclinic feldspar to microcline.

With few exceptions, the other peraluminous, biotite-bearing specimens contain perthitic intermediate microcline (Table 3, Fig. 8) but no sign of orthoclase. In specimen N75 (Table 1, A/CNK = 1.12), a weakly porphyritic granite, both phenocrysts and groundmass contain intermediate microcline (t_1O = 0.85, $\triangle$ = 0.81). Light grey, medium grained biotite granite N77 (Table 1, A/CNK = 1.04) also contains turbid intermediate microcline (t_1O = 0.84, $\triangle$ = 0.71); the diffraction peaks due to albite are considerably sharper than those of microcline because the albite present is more homogeneous in degree of Si–Al order and in composition than is the microcline.

In the friable, coarse grained biotite granites, microcline is clearly subordinate to albite. In N91 (Table 1; A/CNK = 1.13), the microcline has t_1O = 0.86; at a depth of 10 m in borehole L13, t_1O = 0.88; in the specimen taken at 295 m, the microcline approaches more closely an ordered microcline: t_1O = 0.94.

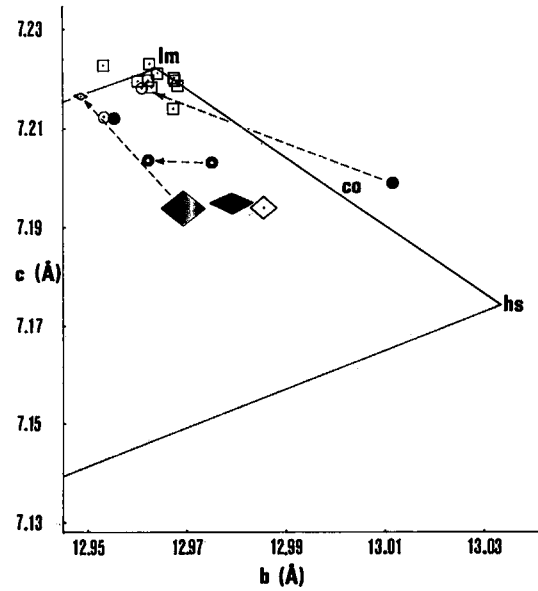

FIG. 8. Plot of the cell dimensions *b versus c* of K-feldspars from the Ririwai rocks, units 2 and 5. Both phenocryst and groundmass in X511 (unit 2) are orthoclases; the phenocryst in N96 (unit 2) is orthoclase, whereas the groundmass contains microcline. These four feldspars are shown with diamonds expressing $\pm 1\sigma$ in *b* and *c*. For clarity, all other points are drawn as circles [closed: phenocryst in biotite granite N94 (unit 5); open: adjacent matrix)] and squares (equigranular biotite granite). Standard errors are generally smaller in triclinic feldspars than in orthoclases. The K-feldspars in X511, N96 and N94 plot in positions that do not agree with *a* observed; these anomalies may be due to strained lattices in cryptoperthitic intergrowths. Stars: coexisting orthoclase and microcline in perthitic amazonite in pegmatitic clot (77–157).

The persistence of orthoclase ($t_1O = t_1m$ = 0.42) in amazonite in pegmatite specimen 77–157 may reflect the large size of the crystals. The amazonite also contains intermediate microcline (minor; t_1O = 0.79, $\triangle$ = 0.50) and ordered albite. The amazonite is cross-cut and rimmed by yellowish intermediate microcline perthite (t_1O = 0.86, $\triangle$ = 0.76) free of orthoclase and in which the albite component predominates (Fig. 4).

Ordered microcline does occur in the microgranite bands encountered in borehole L13 (*e.g.*, at 95 m: t_1O = 1.00, $\triangle$ = 0.92), but is clearly subordinate to albite (Fig. 4). The higher degree of Si–Al order in the microclines may reflect protracted hydrothermal activity, suggesting that these bands represent channelways developed along horizontal joints in the coarse biotite granites. In specimens taken at depths of 411 and 445 m in borehole L13, well-ordered albite (t_1O = 0.98, 0.97, respectively) occurs as a pseudomorph of an original K-bearing feldspar (Fig. 7). The complete replacement of K by Na at such depths may indicate 1) slightly higher temperatures, 2) the longer durations of the interaction with water along the channelways, or 3) the increased alkalinity of the latest fluids to percolate along the joints.

Pink biotite granite (specimen N66), a few centimetres from the greisen, contains turbid intermediate microcline (t_1O = 0.91, $\triangle$ = 0.79) and ordered albite in subequal amounts. In the reddened zone adjacent to the cassiterite-bearing quartz vein and greisen, the microcline is very turbid, free of albite and closer to complete Si–Al order (t_1O = 0.95, $\triangle$ = 0.93). Detailed XRD patterns reveal no trace of breakdown products of microcline [such as kaolinite and sericite, as proposed by Abaa (1976, 1978)]; the intense turbidity reflects the presence of hematite-lined fluid inclusions and vacuoles (Martin & Lalonde 1979).

The vuggy episyenite found in outcrop near the greisen zone (77–169) contains relatively well-ordered intermediate microcline (t_1O = 0.92, $\triangle$ = 0.89) and minor albite in perthitic intergrowth. Specimen 77–160, possibly a variant of the episyenite in which the vugs are filled with sphalerite, contains reddish low microcline (t_1O = 0.97, $\triangle$ = 0.95) without a trace of albite. Thus in the temperature interval 400–250°C, in which cassiterite and sphalerite are deposited (Bowden & Kinnaird 1978), K-bearing aqueous complexes also seem to become supersaturated, resulting in the replacement of albite by K-feldspar.

In terms of a plot t_1O–t_1m–($t_2O + t_2m$) (Fig. 9), the K-feldspars from Ririwai show a remarkable spread in degree of Si–Al order, from orthoclase of varying degrees of order (in unit 2, mainly) to intermediate microclines to fully ordered microcline in the texturally and compositionally most evolved rocks. Such heterogeneity in a granitic pluton had not been documented before; it presumably is typical of near-surface intrusive complexes that have cooled relatively quickly, and that have interacted to various extents with a circulating aqueous fluid phase, not necessarily characterized by constant alkalinity. Note that in most cases, the feldspars followed a path of ordering intermediate between the one-step (Al directly into t_1O, as in albite) and two-step schemes (Al completely in t_1 sites, then in t_1O at the expense of t_1m). However, some specimens of intermediate microcline, apparently devoid of Al in t_2O or t_2m

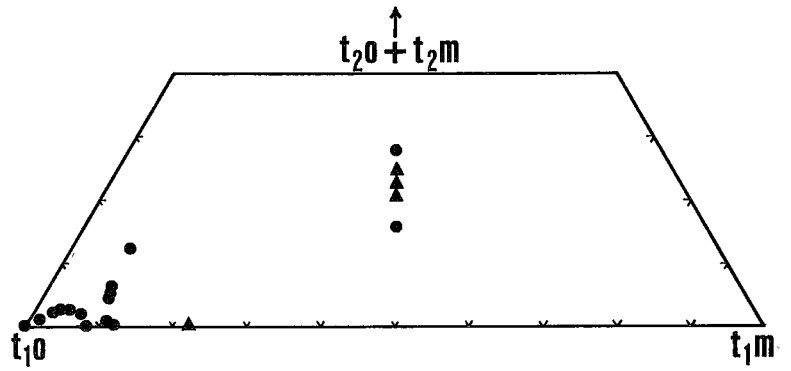

FIG. 9. Plot of tetrahedral Al occupancies t_1O, t_1m, and t_2O+t_2m in the K-rich feldspars of selected Ririwai rocks. Unit 2: triangles; unit 5: circles. Orthoclase is characterized by $t_1O = t_1m$. Most microclines encountered at Ririwai are imperfectly ordered.

(Fig. 9), suggest that the two-step mechanism may have been followed in certain environments characterized by slower cooling and unusual abundance or persistence of a fluid phase. The progression of the ordering process through intermediate steps to fully ordered microcline in potassium-rich environments (*e.g.*, N66 red, 77–160) contradicts the bond-strength-based predictions of Ferguson (1979) concerning the low-temperature stability of orthoclase in such bulk compositions.

The Micas

The main mineralogical expression of peraluminous character in these nonorogenic biotite granites is a trioctahedral mica whose composition falls close to the join between annite $[K_2Fe^{2+}{}_6(Al_2Si_6O_{20})(OH,F)_4]$ and zinnwaldite $[K_2Li_2Fe^{2+}{}_2(Al,Fe^{3+})_2(Al_2Si_6O_{20})(F,OH)_4]$. Preliminary microprobe data for Ririwai micas are shown in Figure 10, a plot of octahedrally coordinated Al as a function of total iron expressed as FeO (J. Kinnaird and C.A. Abernethy, pers. comm. 1980). Also shown in Figure 10 is a zinnwalditic mica from the greisen zone at Ririwai (Jacobson *et al.* 1958, Table V); this mica is olive green and contains 19.6 wt. % Al_2O_3, 1.9% Li_2O, OH and F in roughly equal proportions, and almost no Mg. These aluminous micas, tentatively attributed a postmagmatic origin on the basis of textural information, are zoned outward in Al (and presumably in Li) in N75 and N91, two rocks that contain signs of albitization. In their very high bulk Fe/Mg ratios, these micas strongly reflect the original bulk composition of the granites, and contrast markedly with the more magnesian postmagmatic micas from mineralized episyenites and leucogranites of calc–alkaline affinity. Note that, unlike situations in many calc–alkaline suites, the rocks are free of sericite or secondary muscovite, an indication of the relatively high activity of the alkalis at the hydrothermal stage (*cf.*, Hemley & Jones 1964). The only other important aluminous phase, topaz, is restricted to greisenized granites, which are more aluminous than the adjacent granites (Fig. 2) because of net removal of alkalis.

The Compositional Spectrum of Units 2 and 5

Information on mineralogy and textural evolution of alkali feldspars and micas can be used to rank the rocks of unit 5 (Fig. 4); some of these rocks are acknowledged as being close in composition to the products of magmatic crystallization, whereas many others represent the results of at least one or two distinct waves of metasomatism that accompanied the two episodes of mineralization. In the light of the min-

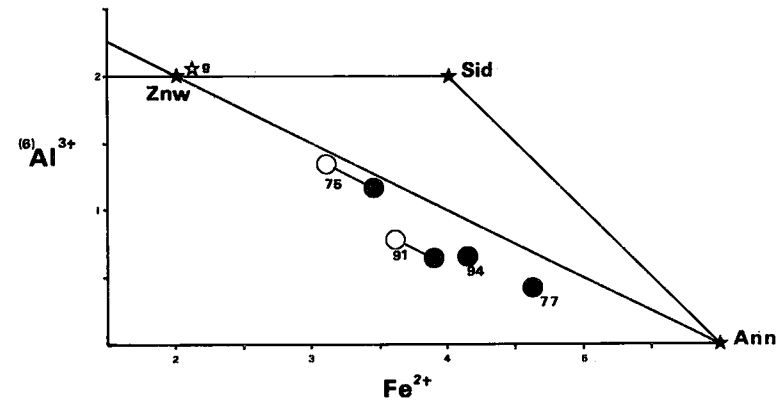

Fig. 10. Compositions of the aluminous trioctahedral micas found in unit 5, expressed in terms of octahedrally coordinated Al and Fe^{2+}. This diagram, developed by C.A. Abernethy (pers. comm. 1980), shows the positions of end-member annite (Ann), zinnwaldite (Znw) and siderophyllite (Sid). The white star refers to a zinnwalditic mica from the greisen zone in the Ririwai lode (Jacobson & MacLeod 1977, Table 8). Closed circles describe the bulk composition of micas in N77 and N94; the core compositions of mica flakes in N75 and N91 are clearly less aluminous than the filamentous rims (closed and open circles, respectively). Microprobe data from J.A. Kinnaird & P. Bowden (in prep.).

eralogical variations noted, we now examine the compositional spectrum of unit-5 rocks in a different projection from that in Figure 2; there, it was seen that most biotite granites analyzed are more aluminous and apparently richer in SiO_2 than X511 and N96 of unit 2. The two quartz-depleted rocks from deep parts of borehole L13 have clearly become peralkaline, whereas the greisenized biotite granite specimens plot very close to the SiO_2 apex, on the aluminous side. The same analyses, taken from Table 1, Abaa (1976) and Jacobson & MacLeod (1977), are plotted in terms of normative constituents Q, Ab and Or (Fig. 11). None of these rocks plots very far off this compositional plane (*e.g.*, Table 1). The simplified trends in the inset diagram illustrate our interpretation of the sequence of metasomatic changes imposed on the original granites.

We consider X511 and N96 (closed circles in Figs. 2 and 11) to closely represent, once the incipient metasomatic effects are removed, the relatively anhydrous magmas that rose to occupy the ring fracture and former vent areas upon cauldron subsidence. The large mass of unit 5, which was stratigraphically at a similar or somewhat lower level in the magma reservoir than the unit-2 material, is unlikely to have been compositionally more evolved (*i.e.*, closer to the minimum in the granite system) than the magma represented by X511 and N96. This inference rests on the assumption that the Ririwai complex does represent a single exhumed igneous centre and that, in agreement with vertical zonation patterns inferred in the magma reservoirs in many other subvolcanic complexes, the magma chamber was zoned in most constituents, including H_2O. Enrichment in dissolved water near the roof explains the early ignimbritic units (Fig. 1b), preserved owing to cauldron subsidence.

If the inference of a zoned magma reservoir is correct, the composition of the granitic liquid responsible for unit-5 rocks would be expected to plot near (possibly slightly below) the closed circles in Figure 11. No such compositions were encountered. Syenitic liquids do form part of the nonorogenic evolutionary trend in the ring complexes of Nigeria and Niger; however, it is in the older, more deeply dissected com-

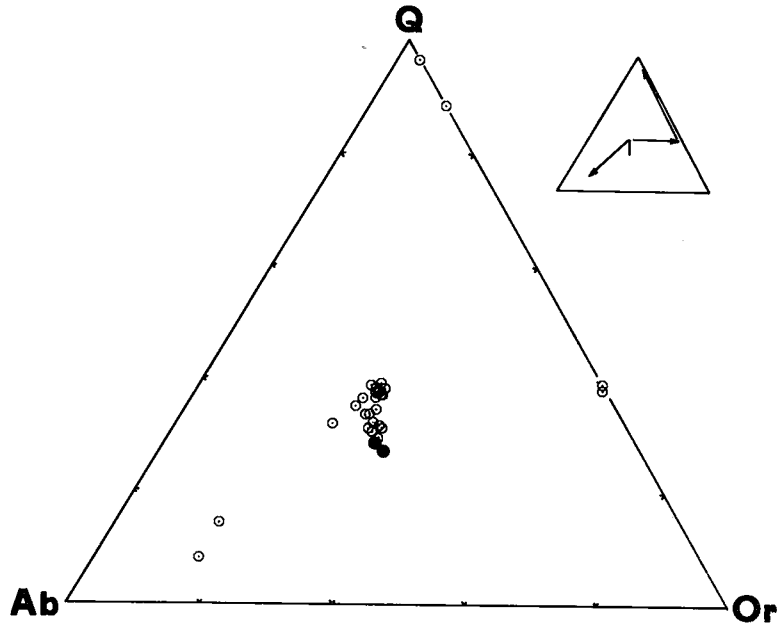

FIG. 11. All analyses of Ririwai biotite granite and metasomatized variants (unit 5), plotted in terms of normative constituents *Q*, *Ab* and *Or*. All rocks plot very close to this compositional plane (see D.I. values in Table 1). Shown for reference as closed circles are X511 and N96 from unit 2 (see text). Sources of data: Jacobson & MacLeod (1977), Abaa (1976), Table 1 and unpublished analyses. Inset: summary of main post-magmatic transformations, culminating in greisen formation (compositions near *Q* apex) between 400 and 250°C.

plexes to the north that indications of these more primitive liquids can be found. We conclude that the array of biotite granite compositions in which Na $\simeq$ K (Fig. 11), all more silicic than the samples of unit 2, arose as a result of minor postmagmatic enrichment in quartz or net removal of the feldspars by dissolution (or both). Dissolution of feldspars must have been incongruent (*e.g.*, Currie 1968), to explain the development of a peraluminous trend (Fig. 2). The aqueous fluid responsible for these changes may have been *relatively* close to neutrality and *relatively* dilute. The bulk compositions so derived contain up to 40% normative quartz (short vertical segment of the bent arrow in the inset, Fig. 11). The circulation of sodium-enriched, more concentrated fluids of alkaline character along dominantly horizontal cooling joints in the mildly albitized biotite granite then led to localized efficient dissolution of K-feldspar and quartz and to the generation of acmite-normative albitites (tip of bent arrow in the inset, Fig. 11). Later, and from the same point of SiO_2 enrichment attained in the mildly albitized biotite granites, complete K-for-Na ion exchange occurred next to east–west vertical joints, leading to the compositions now on the Or–Q join. The tin- and zinc-bearing fluids may also have had the power to remove SiO_2 locally; this would explain the microclinite specimens that have been encountered (not analyzed). Alternatively, the feldspathic rocks may have arisen by efficient ion-exchange of the alkalis in albitites associated with the earlier episode of metasomatism and mineralization. Near the quartz veins, the biotite granites are strongly greisenized, leading to the extreme compositions shown near the quartz apex.

Discussion

A detailed investigation of representative specimens from the "normal" series at Ririwai reveals a spectrum of granitic rocks that illustrate important postmagmatic adjustments in texture and mineralogy. Jacobson (1947), Jacobson *et al.* (1958) and Jacobson & MacLeod (1977) fully recognized the late textural modifications; except in the case of the greisens, however, these investigators did not link the modifications in any systematic way with disturbances in bulk composition of the rocks. On the basis of our preliminary integrated survey of rock compositions, mineralogy and textures, we suggest that rocks of unit 5 (1) generally are disturbed compositionally and (2) can be ranked in order of increasing departure from an original (*i.e.*, magmatic) assemblage. This original assemblage may have been slightly less evolved than the compositions encountered in unit 2. Bulk-composition data for the feldspars have been combined with textural information to formulate the ranking proposed in Figure 4; note that a somewhat different order among the peraluminous granites would emerge if mica composition should be used as a criterion (Fig. 10). The changes imposed at moderate to low subsolidus temperatures culminate in compositionally extreme rocks in the mineralized zones. In most of the rocks of unit 5, however, the changes are much more subtle. We contend that the peraluminous, biotite-bearing granites at Ririwai all show such disturbances, results of mild silicification, ion exchange and incongruent dissolution of alkali feldspar; this conclusion is not intended to imply that peraluminous granitic *liquids* have not been produced in other magmatic centres in the province. The reactions that produce an aluminous biotite probably involved the following reactants: Al and K largely from the feldspar being modified, Fe from the pre-existing mafic mineral assemblage, and Li, F and Na from the near-neutral fluid medium responsible for widespread albitization.

Considered directly relevant to the question of the evolution of biotite granites at Ririwai are the following findings: (1) the progression orthoclase + albite $\rightarrow$ orthoclase + intermediate microcline + albite $\rightarrow$ intermediate microcline + albite $\rightarrow$ low microcline + albite. The presence of microcline implies temperatures of formation below 450°C (Smith 1974, Fig. S–1). The prevalence of intermediate forms of microcline implies that there was insufficient time for equilibrium to be attained in this near-surface environment. (2) The progressive enrichment in Na at the expense of K during the structural conversions listed in (1). (3) The progressive buildup in Si and Al and the overall depletion of alkalis in the granites during the same structural conversions. Could these alkalis have been transferred to the roof rocks, there to metasomatize large volumes of porphyry and ignimbrite? (4) The progressive breakdown of primary, Fe^{2+}-bearing mafic minerals where exposed to circulating fluids, and their preservation where mantled by nonturbid, cryptoperthitic feldspar. (5) The progressive departure of micas from annitic compositions towards Li-, Al-, F-rich trioctahedral micas. The experimental studies of Rutherford (1969) show that the assemblage annite + quartz + two feldspars cannot crystallize from H_2O-saturated granitic

liquids at high crustal levels. This assemblage is stable only below 600°C, which accounts for the absence of biotite as a primary phase in the porphyries of unit 2. Also relevant to point (5) is the absence of volcanic equivalents of the aluminous granites, the albitites and the microclinites.

The changes mentioned above culminated in localized K-for-Na exchange in perthite grains in contact with the lowest-temperature hydrothermal fluid along the east–west system of fractures. The occurrence of K-metasomatism *after* an episode of higher-temperature Na-metasomatism conforms fully to the normal pattern of deuteric adjustments in an epizonal pluton (Burnham 1979). Kinnaird (1979) has used fluid-inclusion studies to document an interval of 400 to 250°C and low salinities of the fluid phase for the episode of cassiterite and sphalerite mineralization. The quantitative removal of Na from feldspar during this event also suggests a low-temperature reaction: Fournier (1976) showed that at 400°C and low pressures, the feldspar that coexists with a Na-bearing gas phase is essentially Or_{100}. Lagache & Weisbrod (1977) found that, in cases where a supercritical fluid phase unmixes at low pressures, the gaseous component is invariably less sodic than the liquid in the system Or–Ab–KCl–NaCl–H_2O. At Ririwai, such a K-bearing gas phase, out of equilibrium with the wallrocks of the fissure system, can be expected to have removed Na in an effort to reach equilibrium in the new environment. As Lagache & Weisbrod suggested, deposition of the ore minerals may well have been another consequence of the unmixing of a supercritical fluid as it entered a low-pressure regime from below or as it became diluted with a dominantly meteoric component.

The subsolidus changes leading to Sn,Zn mineralization occurred during the cooling of the ring complex. This statement rests on the consistency of the isochrons that have been generated for Ririwai rocks. Recent Rb–Sr measurements on specimens from the zone of wallrock alteration in the biotite granites (Bonin *et al.* 1979) yielded an age identical to those previously published. The Rb–Sr isotopic system evidently did not close until after the period of vein-controlled mineralization.

The initial $^{87}Sr/^{86}Sr$ ratio associated with the 10-point isochron (van Breemen *et al.* 1975, Bonin *et al.* 1979) is 0.728 ± 0.007. Such a high value could be taken as strong evidence for the local production of an aluminous granitic magma by partial fusion of the basement, an assemblage of meta-igneous and metasedimentary rocks that yield late Precambrian to Cambrian ages (van Breemen *et al.* 1977). However, one is struck by the scarcity of basement xenoliths in the ring dyke or the biotite granite at Ririwai. One proposal that merits careful consideration concerns the selective leaching of radiogenic strontium from basement rocks near the contact, at the hydrothermal stage. As nonorogenic granites contain little Sr and as most of the strontium is located in feldspar, which is undergoing major transformations that involve dissolution and ion exchange in an aqueous medium, complete resetting of the ratio $^{87}Sr/^{86}Sr$ at the deuteric stage can be expected if the fluid phase enters the cooling body from outside.

The problem of evaluating the petrogenetic processes that gave rise to the biotite granites is difficult in spite of the geochemical data that have been accumulated so far. The question of the extent to which the geochemical systems are reset at subsolidus temperatures must be evaluated in each case. For example, Bowden *et al.* (1979) suggested that the concentrations of the rare earths in mineralized biotite granites were mainly set during the phase of dispersed Nb–Ta mineralization and pervasive albitization. They further proposed that the Eu-depleted chondrite-normalized pattern typical of Ririwai biotite granite was modified by uniform removal of the rare earths (with the exception of Eu) during greisen formation and potassium metasomatism. An enlightened interpretation of geochemical systems can thus be achieved only by recognition of pristine and disturbed rocks using textural and mineralogical indicators.

In contrast to examples in orogenic suites, peraluminous granites in anorogenic tectonic settings are spatially associated with (and petrogenetically related to) peralkaline granites (Lameyre 1980). Peraluminous granites have been found in a number of cases of anorogenic magmatism (*e.g.*, Taylor 1979, Bonin 1980, Anderson *et al.* 1980). In each of these instances, the extent of autometasomatic reactions may depend critically on the amount, composition and provenance of the circulating fluid phase. In view of the potency of an *alkaline* fluid medium as a solvent, the geochemical lines of evidence favoring fractional crystallization, anatexis of sial, and contamination processes will have to be interpreted with caution.

Acknowledgements

We acknowledge the assistance of fellow members of the Nigerian Younger Granite re-

search team, and in particular C.A. Abernethy, J.N. Bennett, J.A. Kinnaird and Richard Batchelor. We thank Professor E.K. Walton for his support. The work forms part of a research project funded by the Overseas Development Ministry (London), grant *R*2679 to P. Bowden. R.F. Martin acknowledges a travel grant from the National Research Council of Canada and the continuing support of the Natural Sciences and Engineering Research Council (grant *A*7721). S.J. Horsky provided some of the X-ray-diffraction patterns. Messrs. J. Allen (University of St. Andrews) and Richard Yates (McGill University) helped with drafting and photography. The cooperation of Dr. Christian N. Okezie and Mr. John A. Adekoya of the Geological Survey of Nigeria led to a productive day in Kaduna. The specimen of microclinite (77–169), from a small hill southwest of Kelly's Dam, is a gift from Mr. David Hanneford, then mine manager of Ririwai Mines Ltd. Ms. V. Trimarchi typed the manuscript.

References

ABAA, S.I. (1976): *Geochemistry and Petrology of Mineralisation at Ririwai, Gindi Akwati and Dutsen Wai in the Nigerian Younger Granite Province.* M.Sc. thesis, Ahmadu Bello Univ., Zaria, Nigeria.

——— (1978): Some geochemical and petrographic aspects of mineralisation in the Ririwai biotite granite, Nigeria. *Ahmadu Bello Univ. Dep. Geol. Bull.* **1**, 1-18.

AJAKAIYE, D.E. (1968): A gravity interpretation of the Liruei Younger Granite ring complex of northern Nigeria. *Geol. Mag.* **105**, 256-263.

ANDERSON, J.L., CULLERS, R.L. & VAN SCHMUS, W.R. (1980): Anorogenic metaluminous and peraluminous granite plutonism in the Mid-Proterozoic of Wisconsin, U.S.A. *Contr. Mineral. Petrology* **74**, 311-328.

APPLEMAN, D.E. & EVANS, H.T., JR. (1973): Job 9214: indexing and least-squares refinement of powder diffraction data. *U.S. Geol. Surv. Comp. Contr.* **20**.

BENNETT, J.N. (1981): *The Petrology and Mineral Chemistry of the Shira Ring-Complex, Northern Nigeria.* Ph.D. thesis, Univ. St. Andrews, St. Andrews, Scotland.

BLASI, A. (1977): Calculation of T-site occupancies in alkali feldspar from refined lattice constants. *Mineral. Mag.* **41**, 525-526.

BONIN, B. (1980): *Les Complexes Acides Alcalins Anorogéniques: l'Exemple de la Corse.* Thèse Doct. d'Etat, Univ. Pierre-et-Marie Curie, Paris.

———, BOWDEN, P. & VIALETTE, Y. (1979): Le comportement des éléments Rb et Sr au cours des phases de minéralisation: l'exemple de Ririwai (Liruei), Nigéria. *C.R. Acad. Sci. Paris* **289D**, 707-710.

BOWDEN, P., BENNETT, J.N., WHITLEY, J.E. & MOYES, A.B. (1979): Rare earths in Nigerian Mesozoic granites and related rocks. *In* Origin and Distribution of the Elements (L.H. Ahrens, ed.). Pergamon, Oxford.

——— & KINNAIRD, J.A. (1978): Younger granites of Nigeria – a zinc-rich tin province. *Inst. Mining Metall. Trans.* **78B**, 66-69.

———, VAN BREEMEN, O., HUTCHINSON, J. & TURNER, D.C. (1976): Palaeozoic and Mesozoic age trends for some ring complexes in Niger and Nigeria. *Nature* **259**, 297-299.

BURNHAM, C.W. (1979): Magmas and hydrothermal fluids. *In* Geochemistry of Hydrothermal Ore Deposits (H.L. Barnes, ed.; 2nd ed.). Wiley-Interscience, New York.

CURRIE, K.L. (1968): On the solubility of albite in supercritical water in the range 400 to 650°C and 750 to 3500 bars. *Amer. J. Sci.* **266**, 321-341.

FERGUSON, R.B. (1979): Whence orthoclase and microcline? A crystallographer's interpretation of potassium feldspar phase relations. *Can. Mineral.* **17**, 515-525.

FOORD, E.E. & MARTIN, R.F. (1979): Amazonite from the Pikes Peak batholith. *Mineral. Record* **10**, 373-384.

FOURNIER, R.O. (1976): Exchange of Na^+ and K^+ between water vapor and feldspar phases at high temperature and low vapor pressure. *Geochim. Cosmochim. Acta* **40**, 1553-1561.

HEMLEY, J.J. & JONES, W.R. (1964): Chemical aspects of hydrothermal alteration with emphasis on hydrogen metasomatism. *Econ. Geol.* **59**, 538-569.

IKE, C.E. (1979): *The Structure, Petrology and Geochemistry of the Tibchi Younger Granite Ring-Complex, Nigeria.* Ph.D. thesis, Univ. St. Andrews, St. Andrews, Scotland.

JACOBSON, R.R.E. (1947): *The Younger Granite Complex of the Liruei Hills, Nigeria.* Ph.D. thesis, Univ. London.

——— & MACLEOD, W.N. (1977): Geology of the Liruei, Banke and adjacent Younger Granite ring-complexes. *Geol. Surv. Nigeria Bull.* **33**.

———, ——— & BLACK, R. (1958): Ring-complexes in the Younger Granite province of northern Nigeria. *Geol. Soc. London Mem.* **1**.

KARCHE, J.-P. & VACHETTE, M. (1976): Migration des complexes subvolcaniques à structure annulaire du Niger. Conséquences. *C.R. Acad. Sci. Paris* 282D, 2033-2036.

KINNAIRD, J.A. (1979): Mineralization associated with the Nigerian Mesozoic ring-complexes. *Stud. Geol. Univ. Salamanca* 14, 189-220.

LAGACHE, M. & WEISBROD, A. (1977): The system: two alkali feldspars–KCl–NaCl–H_2O at moderate to high temperatures and low pressures. *Contr. Mineral. Petrology* 62, 77-101.

LAMEYRE, J. (1980): Les magmas granitiques: leurs comportements, leurs associations et leurs sources. *In* Livre Jubilaire. *Soc. Géol. France, Mém. hors-série* 10, 51-62.

LEROY, J. (1978): The Margnac and Fanay uranium deposits of the La Crouzille district (western Massif Central, France): geologic and fluid inclusion studies. *Econ. Geol.* 73, 1611-1634.

MARTIN, R.F. & LALONDE, A. (1979): Turbidity in K-feldspars: causes and implications. *Geol. Soc. Amer. Abstr. Programs* 11, 472-473.

OLAREWAJU, V.O. (1978): On the basement complex geology of 1:100,000 sheet 126, Ririwai, northern Nigeria. *Ahmadu Bello Univ. Dep. Geol. Bull.* 1, 63-96.

RUTHERFORD, M.J. (1969): An experimental determination of iron biotite – alkali feldspar equilibria. *J. Petrology* 10, 381-408.

SMITH, J.V. (1974): *Feldspar Minerals. 1. Crystal Structure and Physical Properties.* Springer-Verlag, New York.

SMITH, R.L. & BAILEY, R.A. (1968): Resurgent cauldrons. *Geol. Soc. Amer. Mem.* 116, 613-662.

STEWART, D.B. & WRIGHT, T.L. (1974): Al/Si order and symmetry of natural alkali feldspars, and the relationship of strained cell parameters to bulk composition. *Soc. franç. Minéral. Crist. Bull.* 97, 356-377.

TAYLOR, R.P. (1979): Topsails igneous complex – further evidence of middle Paleozoic epeirogeny and anorogenic magmatism in the northern Appalachians. *Geology* 7, 488-490.

TURNER, D.C. & BOWDEN, P. (1979): The Ningi–Burra complex, Nigeria: dissected calderas and migrating magmatic centres. *J. Geol. Soc. London* 136, 105-119.

VAN BREEMEN, O., HUTCHINSON, J. & BOWDEN, P. (1975): Age and origin of the Nigerian Mesozoic granites: a Rb-Sr isotopic study. *Contr. Mineral. Petrology* 50, 157-172.

———, PIDGEON, R.T. & BOWDEN, P. (1977): Age and isotopic studies of some Pan-African granites from north-central Nigeria. *Precambrian Res.* 4, 307-319.

Received June 1980, revised manuscript accepted November 1980.